

## Latest Three-Flavor Neutrino Oscillation Results from NOvA

---

**M. J. Frank<sup>a,\*</sup> on behalf of the NOvA collaboration**

<sup>a</sup>*University of South Alabama*

*E-mail:* [mfrank@southalabama.edu](mailto:mfrank@southalabama.edu)

The NOvA experiment is a long-baseline, off-axis neutrino experiment that aims to study the mixing behavior of neutrinos and antineutrinos using the Fermilab NuMI neutrino beam near Chicago, IL. The experiment collects data at two functionally identical detectors, the Near Detector is near the neutrino production target at Fermilab; the 14 kt Far Detector is 810 km away in Ash River, MN. Both detectors are tracking calorimeters filled with liquid scintillator which can detect and identify muon and electron neutrino interactions with high efficiency. The physics goals of NOvA are to observe the oscillation of muon (anti)neutrinos to electron (anti)neutrinos, understand why matter dominates over antimatter in the universe, and to resolve the ordering of neutrino masses. To that end, NOvA measures the electron neutrino and antineutrino appearance rates, as well as the muon neutrino and antineutrino disappearance rates. In this talk I will give an overview of NOvA and present the latest results combining both neutrino and antineutrino data.

*The European Physical Society Conference on High Energy Physics (EPS-HEP2023)  
21-25 August 2023  
Hamburg, Germany*

---

\*Speaker

## 1. Introduction

This analysis is based on the same data that was previously presented [1], but uses an alternate statistical approach. The original results were determined using a frequentist approach while the analysis presented here uses a Bayesian Markov Chain technique. Both analyses are based on a total exposure of  $13.6 \times 10^{20}$  POT in neutrino mode and  $12.5 \times 10^{20}$  POT in antineutrino mode [2]. We found the results consistent between the two statistical treatments, and they are given as follows:

$$\begin{aligned}\Delta m_{32}^2 &= 2.41 \pm 0.07 \times 10^{-3} \text{ eV}^2 \\ \sin^2 \theta_{23} &= 0.57_{-0.04}^{+0.03} \\ \delta_{\text{CP}} &= 0.82\pi_{-0.87\pi}^{+0.27\pi}\end{aligned}\tag{1}$$

The Bayesian treatment allows NOvA to measure  $\theta_{13}$  directly without the usual external reactor constraints:

$$\sin^2 (2\theta_{13}) = 0.085_{-0.016}^{+0.020}\tag{2}$$

### 1.1 NOvA

The acronym NOvA stands for NuMI Off-Axis  $\nu_e$ -Appearance, which summarizes our experiment. The NuMI (Neutrinos at the Main Injector) facility provides the muon neutrino ( $\nu_\mu$ ) source. These neutrinos travel north through the earth to the Far Detector (FD) which is located 14 mrad off the beam axis where we expect an almost monoenergetic beam of 2 GeV neutrinos. During their 810 km journey to the FD, the neutrinos (antineutrinos) oscillate in their flavor states and we measure the disappearance rate of muon neutrinos (antineutrinos) and appearance rate of electron neutrinos (antineutrinos). From this we can measure the transition probabilities  $P(\nu_\mu \rightarrow \nu_\mu)$  and  $P(\nu_\mu \rightarrow \nu_e)$  in the neutrino mode, and  $P(\bar{\nu}_\mu \rightarrow \bar{\nu}_\mu)$  and  $P(\bar{\nu}_\mu \rightarrow \bar{\nu}_e)$  in the antineutrino mode. These transition probabilities are functions of the neutrino oscillation parameters, which we can then extract to yield our results (see Eq. 1).

### 1.2 Detector Design

The neutrino interaction cross section is very low, so we require a large detector mass. When an electron neutrino interacts with the detector, an electron is produced that will in turn produce an electromagnetic (EM) shower. We therefore designed a “fully active” detector using low  $Z$  materials. We use PVC extrusions filled with liquid scintillator, which provides a radiation length of approximately 40 cm and a Molière radius of 11 cm. Each of the extrusions contains one wavelength-shifting fiber that is read out by an avalanche photo-diode (APD). This detection technique is optimized to differentiate EM showers from hadronic showers.

### 1.3 Neutrino Beam and Detectors

The neutrinos are created in the NuMI facility by colliding 120 GeV protons on a graphite target, which results in  $\pi^+$  particles that are allowed to decay into  $\mu^+$  and  $\nu_\mu$ . The  $\mu^+$  particles are stopped by muon absorbers and the muon neutrinos travel onward to the Near Detector (ND). The average NuMI beam power for this data period was 650 kW with a peak hourly-average of 756 kW.

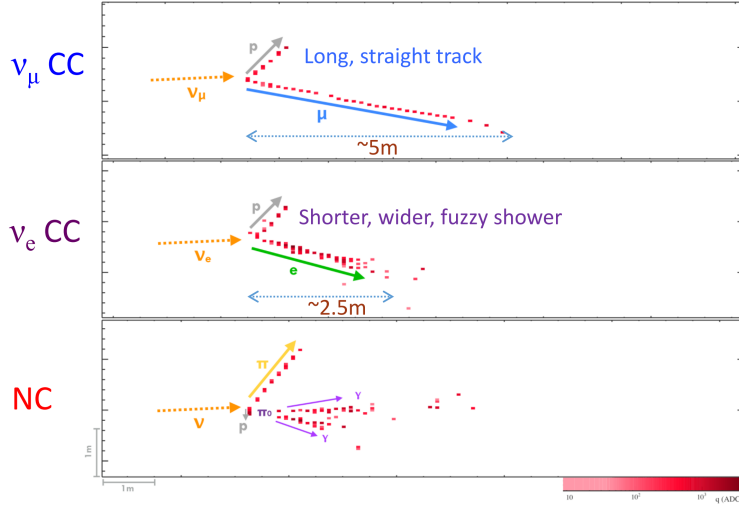


**Figure 1:** Simulated ND event with a visible energy of 2 GeV. The top event shows a  $\nu_\mu$  charged-current interaction with the characteristically long muon track and short proton track with large energy deposition. The middle event shows a  $\nu_e$  charged-current interaction that demonstrates the long EM shower in our “fully active” detector. The bottom event shows a hadronic interaction where the majority of the  $\pi^0$  momentum is carried by one of the two decay photons, which in turn produces a displaced EM shower.

The ND is located 105 m underground and 14 mrad off the beam axis. It has a mass of approximately 300 tons and a size of 4 m by 4 m by 15 m. The FD is located on the surface a distance of 810 km away and also 14 mrad off the beam axis. Its construction was completed in 2014 and it has a mass of over 14,000 tons and a size of 15 m by 15 m by 60 m.

Figure 1 shows the simulated signatures of different particle interactions in the ND. It shows that we are able to differentiate EM showers (center) from hadronic showers (bottom). With this particle identification we can measure  $P(\nu_\mu \rightarrow \nu_\mu)$  ( $P(\bar{\nu}_\mu \rightarrow \bar{\nu}_\mu)$ ) and  $P(\nu_\mu \rightarrow \nu_e)$  ( $P(\bar{\nu}_\mu \rightarrow \bar{\nu}_e)$ ) by looking for a deficit of  $\nu_\mu$  ( $\bar{\nu}_\mu$ ) events and an excess of  $\nu_e$  ( $\bar{\nu}_e$ ) events, respectively. We can then extract nature’s parameters based on the standard oscillation equations using a baseline of 810 km and a neutrino energy of 2 GeV.

## 2. Neutrino Results

Figure 2 shows the neutrino event counts in the FD for neutrino running on the left and for antineutrino running on the right. The top row gives the electron neutrino event counts as a function of reconstructed neutrino energy and the bottom gives the same for muon neutrinos. The electron neutrino events were separated into three groups of particle identification (PID) quality: high, low, and peripheral. Figure 3 shows the corresponding transition probabilities divided into two energy bins. The nearby ellipses show the theoretical values of the transition probabilities for all values of  $\delta_{CP}$  for both the normal (blue) and inverted (yellow) neutrino mass ordering. As can be seen, NOvA’s data falls near the center between the two ellipses, which makes resolving the oscillation parameters difficult. Another way to look at this is by plotting the neutrino-antineutrino event asymmetry as a function of reconstructed energy, which is shown in Figure 4. The data shows that NOvA measures an event asymmetry close to zero, so we see as many neutrino as antineutrino

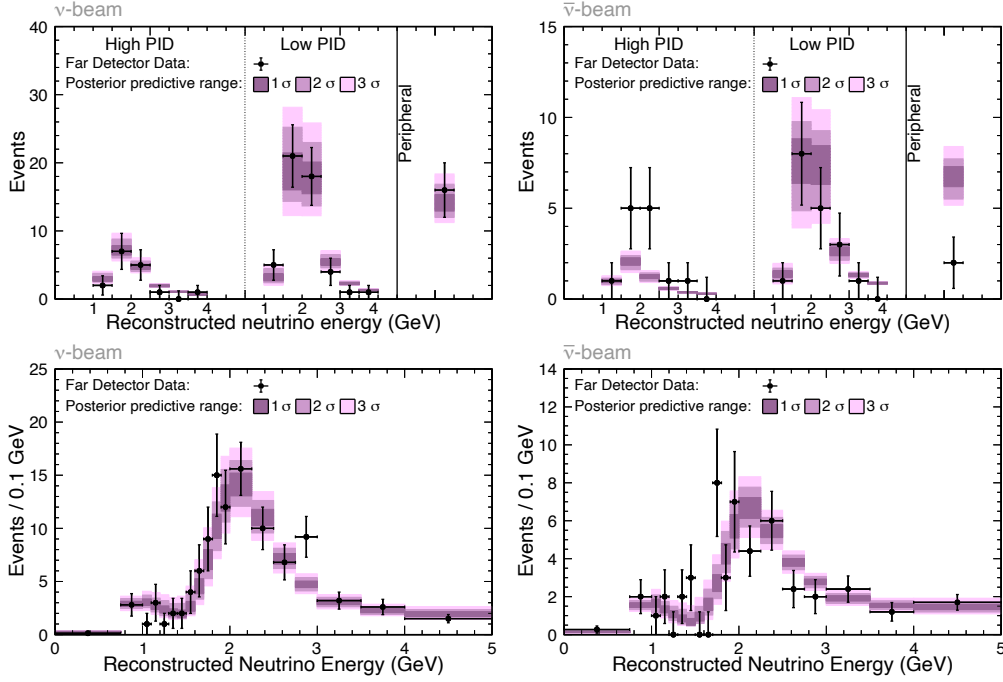


**Figure 2:** Neutrino event counts as a function of reconstructed neutrino energy for electron neutrinos (top) and muon neutrinos (bottom) in neutrino mode (left) and antineutrino mode (right). The electron neutrino events were separated into three groups of particle identification (PID) quality: high, low, and peripheral.

events. The dashed black line in Figure 4 shows the neutrino event asymmetry measured by T2K, which is larger.

The event counts from Figure 2 are re-analyzed using a Bayesian technique implementing a Markov Chain integrator. The advantage of this framework is that parameters and their confidence intervals can be directly inferred by integrating the posterior distributions. This expands the neutrino oscillation parameters that NOvA can comment on, as for example a direct measurement of  $\theta_{13}$ , which is usually constrained externally. Another example is the determination of the Jarlskog invariant, which is a measure of the amount of CP-violation; a value of zero corresponds to no CP violation. Figure 5 (right) shows the posterior probability density of the Jarlskog invariant together with the Bayesian confidence intervals for the normal mass hierarchy (top) and inverted mass hierarchy (bottom). The zero point is excluded at the 1-2 $\sigma$ -level for the normal ordering and at around the 3 $\sigma$ -level for the inverted hierarchy. The left plot in Figure 5 shows the Bayesian results for the  $\sin^2(\theta_{23})$ - $\delta_{CP}$  allowed phase space for the normal mass hierarchy (top) and the inverted mass hierarchy (bottom). These results are consistent with the frequentist interpretation of the data.

### 3. Conclusion

Figure 6 shows NOvA’s projected significance of discovering CP violation (left) and significance of resolving the mass ordering (right) as a function of POT. While crossing the 3- $\sigma$  threshold is difficult with the data that we have and that we plan to take, we hope to significantly narrow the

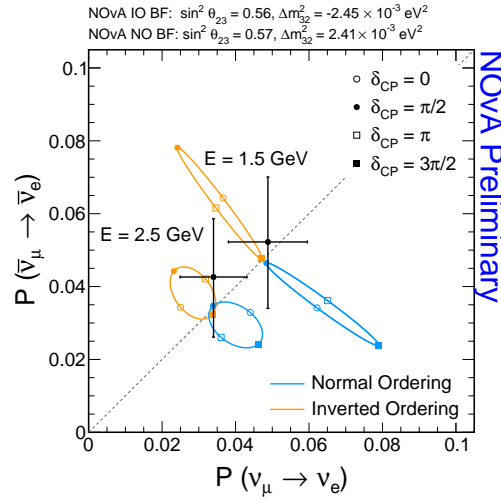


**Figure 3:** This plot shows the transition probabilities  $P(\nu_\mu \rightarrow \nu_e)$  and  $P(\bar{\nu}_\mu \rightarrow \bar{\nu}_e)$  for different values of  $\delta_{CP}$  for the normal (blue ellipse) and inverted (yellow ellipse) mass hierarchies. The NOvA measurements are divided into two energy bins (1.5 GeV and 2.5 GeV) and superimposed.

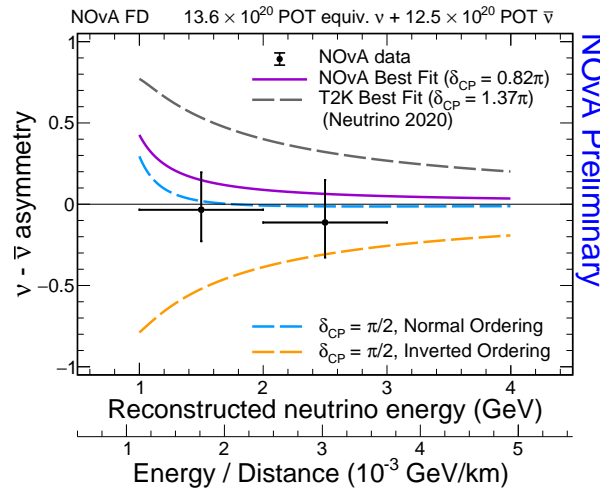


**Figure 4:** Neutrino-antineutrino event asymmetry as a function of reconstructed neutrino energy with the NOvA best fit shown in purple. The theoretical asymmetries are included for the normal mass hierarchy (blue) and the inverted mass hierarchy (yellow) for  $\delta_{CP} = \frac{\pi}{2}$ . The T2K best fit results (black dashed) are included for comparison.

allowed phase space bands from Figure 5. As of now, NOvA is scheduled to run at least through 2026, which is already six years beyond the original design plans.

## Acknowledgments

This document was prepared by the NOvA Collaboration using the resources of the Fermi National Accelerator Laboratory (Fermilab), a U.S. Department of Energy, Office of Science, HEP User Facility. Fermilab is managed by Fermi Research Alliance, LLC (FRA), acting under Contract No. DE-AC02-07CH11359. This work was supported by

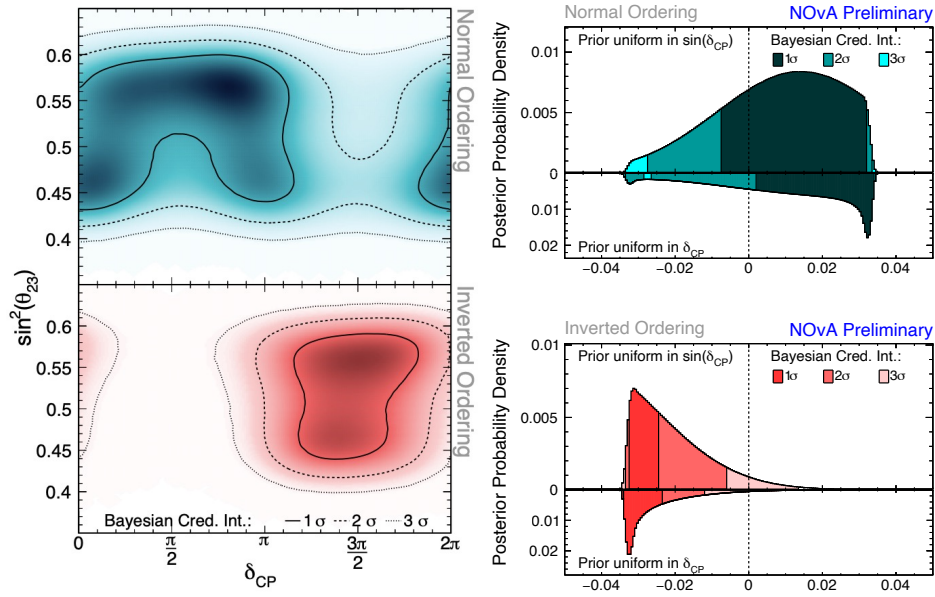


**Figure 5:** Bayesian results for the oscillation parameters (left) and the Jarlskog invariant (right) for the normal mass ordering (top/blue) and the inverted mass ordering (bottom/red). The Jarlskog invariant is shown for two separate prior assumptions as indicated on the plots. A Jarlskog invariant of zero corresponds to no CP violation.

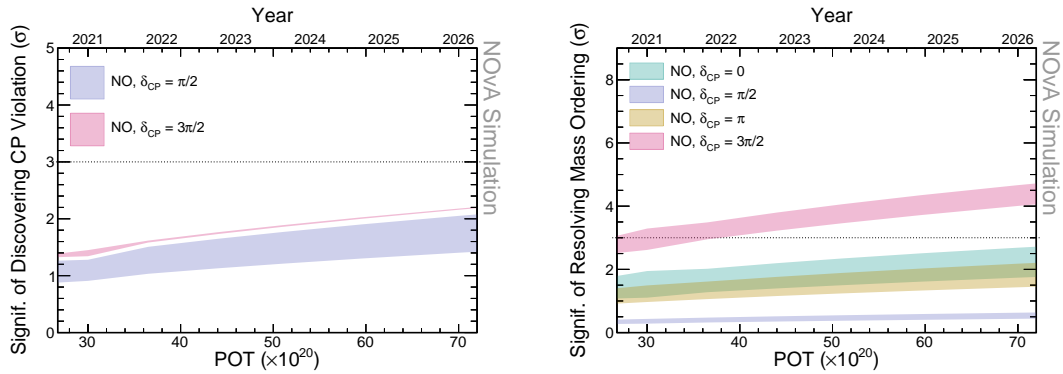


**Figure 6:** NOvA projections of discovering CP violation (left) and resolving the mass ordering (right) as functions of POT and year.

the U.S. Department of Energy and the U.S. National Science Foundation; the Department of Science and Technology, India; the European Research Council; the MSMT CR, GA UK, Czech Republic; the RAS, MSHE, and RFBR, Russia; CNPq and FAPEG, Brazil; UKRI, STFC, and the Royal Society, United Kingdom; and the state and University of Minnesota. We are grateful for the contributions of the staffs of the University of Minnesota at the Ash River Laboratory and of Fermilab.

## References

- [1] S. Calvez *et al.* (NOvA Collaboration), PoS (EPS-HEP2021) 233 (2022).
- [2] M. A. Acero *et al.* (NOvA Collaboration), *Phys. Rev. D* **106**, 032004 (2022).